



Significant catalytic recovery of spent industrial DuPont catalysts by surface deposition of an amorphous vanadium-phosphorus oxide phase

Raquel Mateos Blanco^{a,*}, Ali Shekari^b, Silvia González Carrazán^c, Elisabeth Bordes-Richard^d, Gregory S. Patience^b, Patricio Ruiz^a

^a Université Catholique de Louvain, Louvain-la-Neuve 1348, Belgium

^b Genie Chimique, École Polytechnique de Montréal, Canada

^c Universidad de Salamanca, Salamanca 37008, Spain

^d Université des Sciences et Technologies de Lille, Villeneuve d'Ascq 59655, France

ARTICLE INFO

Article history:

Received 9 January 2012

Received in revised form 1 March 2012

Accepted 3 April 2012

Available online 4 June 2012

Keywords:

Industrial DuPont catalyst

VPO phases

Reactivation

ABSTRACT

DuPont's vanadium phosphorous oxide catalyst (VPO) deactivated with time-on-stream in a commercial butane to maleic anhydride reactor. Coincidentally, V^{5+} phases formed on the surface (based on XPS) – principally β -VOPO₄ but also V₂O₅. This catalyst was reactivated by introducing a small amount of a VPO (theoretical P/V atomic ratio = 0.86) phase. The maleic anhydride production rate of the reactivated catalyst was higher by about 60% compared to the used catalyst. *n*-Butane conversion increased by about 50% and the selectivity to maleic anhydride improved by 15%. The analyses of the modified catalyst by X-ray diffraction, Raman spectroscopy and X-ray photoelectron spectroscopy showed that the V₂O₅ and β -VOPO₄ phases disappeared and suggested that an amorphous phase formed on the surface. The treatment resulted in a lower V^{5+}/V^{4+} and P/V ratios on the used catalyst surface.

© 2012 Elsevier B.V. All rights reserved.

1. Introduction

Some efforts have been made to study the deactivation and/or the regeneration of VPO catalysts during the last 40 years. Attempts have been made to protect VPO catalysts against deactivation by using metal promoters [1]. The kinetics of reoxidation of the selective vanadyl pyrophosphate (VPP) phase have also been studied, but no catalytic performance after such a treatment have been reported [2]. The deactivation of doped or supported VPO catalysts during the oxidation of *n*-butane to maleic anhydride has been attributed to modifications of their properties depending on the process conditions (pressure, temperature, molar concentrations of *n*-butane and air and type of reactor). The deactivation mechanisms may include the crystallization of amorphous phase(s), the accumulation of carbonaceous species on the surface, the over-reduction (V^{4+} into V^{3+} sites) or over-oxidation (V^{4+} into V^{5+} sites) of vanadium, the loss of phosphorus and the agglomeration or sintering of the catalyst surface during relatively long oxidation periods [3–6]. A proper combination of the oxidation states of the surface vanadium species, or an optimal V^{4+}/V^{5+} ratio, were related to high activity and selectivity, as well as a P/V atomic ratio slightly higher than 1.0. Another determining factor in VPO catalyst activity is the P/V

ratio on the catalyst surface, which is related to the mean oxidation state of vanadium, the higher the value the lower the trend for VPP over-oxidation [7–9]. An excessive oxidation and/or high temperature (as in hot spots typical of fixed bed reactors) could also result in catalyst deactivation by means of the gradual transformation of surface amorphous layers into crystalline VOPO₄ phases [10,11]. Typically, the P/V = 1.02 in the DuPont catalyst was chosen to avoid over-reduction in the recirculating solid riser reactor [12,4].

The following bases were considered for the strategy to study the reactivation of VPO spent catalyst. (i) *The dynamics of VPO catalysts*. The oxidation state of vanadium as well as the structure of catalyst surface adapt to the prevailing red/ox C₄/O₂ conditions [13–18]. The catalytic properties of the fresh catalyst are thus modified during the “equilibration” period [8], which may take weeks in industrial reactors [16], before the actual steady state is reached. During that period, the bulk composition and/or structure may be modified accordingly. (ii) *The multiphase composition of the catalysts*. It is well known from the literature, that besides crystalline (VO)₂P₂O₇, which is the major phase, a variety of VOPO₄ (α , δ , γ) phases have been observed. (iii) *The VPO location*. The VPO active sites are, seemingly, displayed as a thin amorphous layer on the top of (VO)₂P₂O₇ [13–15]. (iv) *The oxidation state of vanadium*. On the surface, the two oxidation states, V^{5+} and V^{4+} , of vanadium were associated with high catalytic performance, V^{5+} species being necessary to oxidize the intermediates to MA, besides V^{4+} species for activation of *n*-butane as well as of dioxygen. (v) *The exact nature*

* Corresponding author.

E-mail address: raquel.mateos@live.com (R.M. Blanco).

of the active sites, considered to be made of dispersed V^{5+} on the surface of $(VO)_2P_2O_7$, or of $VOPO_4$ microdomains coexisting with $(VO)_2P_2O_7$. (vi) A synergetic effect due to the cooperation between VPO phases. Coherent interfaces between $VOPO_4$ and $(VO)_2P_2O_7$ owing to their low crystallographic misfit [5,8,9] and surface oxygen migration [19] were proposed. Higher catalytic performance was observed when two catalysts containing different P/V atomic ratio were brought into physical contact [19]. Finally, the surface and bulk reactivities of the catalyst, as well as its crystal morphology to which they are related, depend primarily on the “sample history” (nature of raw materials, method of preparation, heat treatment, activation, etc.) determined by the method of preparation [3,20,21]. This is even the reason why there are so many discrepancies in the literature.

In this work, we rejuvenated spent DuPont VPO catalyst by a treatment resulting in the loading of two monolayers of a VPO phase on its surface. The main properties of this catalyst modified by impregnation with a small amount of a VPO phase were compared to those of deactivated VPO catalyst and their catalytic performance was studied.

Indeed, the deactivation was assumed to be due to the transformation of V^{5+} containing phase(s) during the long time-on-stream exposure (more than 2 years) in the reaction conditions of DuPont's Circulating Fluidized Bed reactor. It was expected that the surface would be restructured, either by regenerating a VPO phase, or by reaching a more appropriate V^{5+}/V^{4+} ratio and P/V ratio.

2. Experimental

2.1. Preparation of catalysts

2.1.1. The DuPont catalysts

The DuPont VPO precursor was prepared on a commercial scale in an organic medium with isobutanol and benzyl alcohol. This step was followed by micronization to 1–2 μm , then spray drying with polysilicic acid to form microspheres resulting in VPO encapsulated in a porous silica shell [22,23].

Two samples were investigated: (i) the precursor, $VOHPO_4 \cdot 0.5H_2O$, denoted as VPO-P catalyst, and (ii) the spent catalyst ($8 \text{ m}^2 \text{ g}^{-1}$) used in DuPont's commercial circulating fluidized bed reactor. This catalyst is denoted as VPO-S. The nominal silica content in VPO-S was 10%.

2.1.2. Phosphorus-vanadium catalyst prepared in isobutanol (VPO-2M)

40 g of V_2O_5 (PANREAC, ref. 17524) was first dissolved in 500 mL of isobutanol (ALFA AESAR, ref. 36643) under reflux and stirred (900 rpm) during 16 h; the resulting suspension was then filtered. In the second step, the filtrate (containing 27.2 wt.% of V) was refluxed and stirred (900 rpm) with H_3PO_4 85% aqueous solution (PANREAC, ref. 18067) during 16 h. The precipitate obtained was filtered and then dried in an oven at 150°C for 20 h [19]. This catalyst is denoted as VPO-2M. The value of P/V atomic ratio was 0.86 as determined by chemical analysis.

2.1.3. VPO-S catalyst modified by 2 monolayers of VPO

A modified spent VPO DuPont catalyst was obtained by suspending its particles in the same type of mixture as the one used to prepare VPO-2M, with an amount corresponding to two theoretical monolayers of VPO-2M (P/V = 0.86). The amount of VPO necessary to form a monolayer was calculated from the specific surface area of VPO-S ($8 \text{ m}^2 \text{ g}^{-1}$) and the area covered by 'a molecule' of (100) layer of $(VO)_2P_2O_7$, assuming that the surface occupied by this molecule is the same as one occupied by a molecule of V_2O_5 (11 \AA^2) [24]. The following procedure was adopted. The filtrate, obtained after

filtering a suspension containing 40 g of V_2O_5 dissolved in 500 mL isobutanol in the same conditions as previously detailed (27.2 wt.% of V), was diluted in 1000 mL isobutanol under stirring. VPO-S particles (20 g) were suspended in a solution containing the amount of vanadium prepared as above to which H_3PO_4 necessary to achieve a P/V ratio = 0.86 was added. The resulting suspension was refluxed and stirred (900 rpm) during 16 h. The solvent was then evaporated under vacuum and the solid was dried in an open oven at 150°C for 20 h. The modified solid is denoted as VPO-S + 2M.

2.1.4. Blank samples

To ensure that the step in isobutanol was not modifying the DuPont sample properties, blank samples were prepared by suspending the VPO precursor (VPO-P) or the spent VPO catalyst (VPO-S) in 20 mL of isobutanol under reflux and stirring (900 rpm) during 16 h. The solvent was evaporated under vacuum and the solid thus obtained was dried in an oven at 150°C for 20 h. Samples are denoted as VPO-P-b and VPO-S-b, respectively. The denotation of all catalytically tested samples is extended by “t”.

2.2. Characterization methods

The VPO-S sample was analysed by X-ray diffraction (XRD) using a Huber diffractometer ($\text{CuK}\alpha$ radiation, $\lambda = 0.15418 \text{ nm}$), in the range $2\theta = 10\text{--}80^\circ$ at room temperature. Lines were attributed using the DIFFRACPlus software (Bruker). All the other samples were characterized using a Siemens D5000 diffractometer ($\text{CuK}\alpha$ radiation, $\lambda = 0.15418 \text{ nm}$).

XPS analyses were performed using a Kratos Axis Ultra spectrometer (Kratos Analytical, UK), equipped with a monochromatized aluminium X-ray source (powered at 10 mA and 15 kV). Charge stabilization was achieved by using the Kratos Axis device. Analyses were performed in the hybrid lens mode with the slot aperture and the iris drive position set at 0.5 inch; the resulting analysed area was $700 \mu\text{m} \times 300 \mu\text{m}$. The pass energy of the hemispherical analyser was set at 160 eV for the wide scan and 40 eV for narrow scans. In the latter conditions, the full width at half maximum (FWHM) of the Ag 3d_{5/2} peak of clean silver reference sample was about 0.9 eV. The sample powders were pressed into small stainless steel troughs mounted on a multi-specimen holder. The pressure in the analysis chamber was 10^{-6} Pa. The photoelectron collection angle θ between the normal to the sample surface and the electrostatic lens axis was 0° . The following sequence of spectra were recorded: survey spectrum, C 1s, O 1s, V 2p, P 2p, Si 2p, N 1s and C 1s again to check for charge stability as a function of time and the absence of sample degradation. The C-(C,H) component of the C 1s peak of carbon was fixed to 284.8 eV to set the binding energy scale. The data was analysed with the Casa XPS software (Casa Software Ltd., UK). The peaks were decomposed using a linear baseline, and a component shape defined by the product of a Gauss and Lorentz function, in a 70:30 ratio, respectively. Molar concentration ratios were calculated using peak areas normalized according to the acquisition parameters and the relative sensitivity factors and transmission function provided by the manufacturer.

Laser Raman spectra (LSR) of all samples were recorded using a Labram Infinity Laser Raman Spectrometer (JY-DILOR) equipped with an optical microscope. The laser intensity (Ar^+ , 514.5 nm) was reduced by various filters (<1 mW), and the data were treated by Labspec software. The spectral resolution and the accuracy of the Raman shifts were evaluated at 2 cm^{-1} .

2.3. Catalytic activity

The catalytic properties were measured in a fixed bed micro-reactor; 400 mg of catalyst were loaded to a 7 mm quartz tube and a reactant mixture was fed at a rate of 40 mL/min (STP). The catalytic

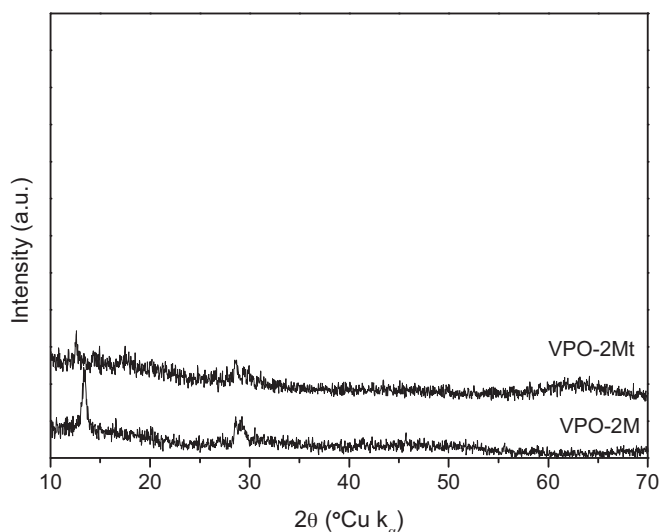


Fig. 1. XRD analysis of sample VPO-2M (before) and VPO-2Mt (after) catalytic testing (after Step 1 + Step 2 + Step 3).

tests were conducted on VPO samples without any particular size adjustment after their preparation. A particle size analysis on the catalyst samples showed an average particle size ranging from 11 to 53 μm for all the samples while 90% of the particles in the majority of samples had a maximum size of 66 μm . Before evaluating the reaction performance, the samples were calcined at 390 °C and 1 atm for 10 h under 21% O_2 in argon. For VPO-2M the test was performed with 100 mg. The operating conditions were: *Step 1*: 380 °C, 1.4% C_4H_{10} , 18.1% O_2 , balance Ar during 120 min; *Step 2*: 400 °C, 1.4% C_4H_{10} , 18.1% O_2 , balance with Ar during 20 min; and finally, *Step 3*: 380 °C, 3.6% C_4H_{10} /13.4% O_2 , balance Ar, during 20 min.

3. Results

3.1. Influence of isobutanol slurring and deposition of 2M on the surface area of catalysts

The specific surface area of VPO-S catalyst increased from 8 $\text{m}^2 \text{g}^{-1}$ to 14 $\text{m}^2 \text{g}^{-1}$ when the catalyst was slurred in isobutanol (blank, VPO-S-b), which was indicative of the existence of a soluble fraction. When VPO-S was slurred in the equivalent of 2 monolayers of P/V = 0.86 (VPO-S+2M), the surface area increased, but less than for VPO-S-b since it was 12 $\text{m}^2 \text{g}^{-1}$. The surface area of the raw DuPont precursor was 14.6 $\text{m}^2 \text{g}^{-1}$.

3.2. Characterization of fresh samples

The XRD pattern of VPO-2M is presented in Fig. 1. The fresh solid before catalytic testing was mainly amorphous, with a few main lines that could be assigned to $(\text{VO})_3(\text{PO}_4)_2 \cdot 7\text{H}_2\text{O}$ (ICDD-JCPDS 49-1257) or $(\text{VO})_3(\text{PO}_4) \cdot 2.9\text{H}_2\text{O}$ (ICDD-JCPDS 48-1200), in accordance with P/V < 1.

The XRD pattern of VPO-S revealed lines belonging to $(\text{VO})_2\text{P}_2\text{O}_7$, $\beta\text{-V}_2\text{O}_5$, β and $\delta\text{-VOPO}_4$, in accordance with Dummer et al. [25] (Table 1). The intensity of the $\beta\text{-V}_2\text{O}_5$ lines was lower in the VPO-S-b pattern that is after slurring it in isobutanol. The disappearance of $\beta\text{-V}_2\text{O}_5$ lines in the XRD pattern of VPO-S+2M was confirmed by Raman spectroscopy. The Raman spectra of VPO-S, VPO-S-b and VPO-S+2M catalysts exhibited the bands of $(\text{VO})_2\text{P}_2\text{O}_7$ and of oxovanadium (V) phosphate phases (Table 1). $\beta\text{-VOPO}_4$ was detected by LRS technique in VPO-S+2M. $(\text{VO})_2\text{P}_2\text{O}_7$ and a mixture of hydrated $\text{VOPO}_4 \cdot 2\text{H}_2\text{O}$ phases were also present, as observed by XRD. Some coke that could be formed from

Table 1

Analyses by laser Raman spectroscopy and X-ray diffraction of samples before (VPO-S, blank VPO-S-b, modified VPO-S+2M) and after catalytic testing experiments (VPO-S-bt and VPO-S+2Mt).

Catalyst	Raman	XRD
VPO-2M		(Amorphous)
VPO-S	$(\text{VO})_2\text{P}_2\text{O}_7$, $\alpha_1\text{-}\beta\text{-}$, $\delta\text{-VOPO}_4 + \text{VOPO}_4 \cdot 2\text{H}_2\text{O} + \beta\text{-V}_2\text{O}_5$	$(\text{VO})_2\text{P}_2\text{O}_7 + \beta\text{-}$, $\delta\text{-VOPO}_4 + \beta\text{-V}_2\text{O}_5$
VPO-S-b	$(\text{VO})_2\text{P}_2\text{O}_7 + \text{VOPO}_4$ ($\alpha_1?$)	Mainly $(\text{VO})_2\text{P}_2\text{O}_7$ ($\beta\text{-V}_2\text{O}_5$ low)
VPO-S-bt	$(\text{VO})_2\text{P}_2\text{O}_7 + \alpha_1\text{-VOPO}_4 + (\text{VOPO}_4 \cdot 2\text{H}_2\text{O})$	$(\text{VO})_2\text{P}_2\text{O}_7 + \beta\text{-V}_2\text{O}_5$
VPO-S+2M	$(\text{VO})_2\text{P}_2\text{O}_7 + \beta\text{-VOPO}_4 + \text{coke}$	$(\text{VO})_2\text{P}_2\text{O}_7 + \text{mixture of hydrated VPO}$
VPO-S+2Mt	$(\text{VO})_2\text{P}_2\text{O}_7 + \beta\text{-VOPO}_4$ ($(\text{VO})_2\text{P}_2\text{O}_7 + \alpha_1\text{-VOPO}_4$)	$(\text{VO})_2\text{P}_2\text{O}_7$

isobutanol after drying was observed by LRS in the VPO-S+2M spectrum (bands centred at about 1600 and 1450 cm^{-1}). An important conclusion is that part of $\beta\text{-V}_2\text{O}_5$ which was formed under reaction conditions in the spent catalyst was probably eliminated upon slurring the catalyst with isobutanol. It could be also that the iron species originating from abrasion of the particles on reactor walls or excess of phosphate were washed away. These results are in accordance with the increase in surface area.

XPS experiments were carried out on precursor and catalysts. The values found for the binding energies of vanadium (Table 2) were typically ascribed to V^{5+} in VOPO_4 and to V^{4+} in $(\text{VO})_2\text{P}_2\text{O}_7$, respectively. The relative amount of V^{5+} and V^{4+} and the P/V atomic ratio depended on the samples. A high amount of V^{5+} (about 40%, $\text{V}^{5+}/\text{V}^{4+} = 0.7$) was present in the ca. 1 nm depth of VPO-2M analysed, while the P/V atomic ratio was ≤ 1.0 (theoretical bulk P/V = 0.86). A high charge effect made it difficult for a more precise analysis of this sample.

In the blank VPO-S-b spent catalyst, the $\text{V}^{5+}/\text{V}^{4+}$ ratio amounted to 1.2 (54% of V^{5+}), which is high, while, as expected, it was low on blank precursor VPO-P-b (7% of V^{5+}). The P/V ratio was remarkably equal to 1/1 in all examined catalysts, except in VPO-S-b (P/V = 1.2). The high fraction of V^{5+} detected in VPO-S-b is in agreement with the fact that VOPO_4 phases (principally $\alpha_1\text{-VOPO}_4$) but also V_2O_5 besides $(\text{VO})_2\text{P}_2\text{O}_7$ were found by XRD and LRS (Table 1). Thus, one of the main reasons for the ageing of this catalyst was the high amount of V^{5+} formed, as well as the presence of V_2O_5 and $\alpha_1\text{-VOPO}_4$. In the VPO-S+2M catalyst, namely when the equivalent of 2 monolayers of VPO (P/V = 0.86) were added to VPO-S, the amount of V^{5+} dramatically decreased to the value observed in VPO-P catalyst (about 10%, $\text{V}^{5+}/\text{V}^{4+} = 0.1$). According to Dummer et al. [25] who

Table 2

XPS analysis of VPO-2M (P/V = 0.86), blank before (VPO-S-b) and after test (VPO-S-bt), and modified before (VPO-S+2M) and after test (VPO-S+2Mt). A% is the percentage of photopeak area of V^{5+} and V^{4+} . Value of A in VPO-P-b: 7%. Binding energies: BE = 518.1–518.4 eV for V^{5+} in VOPO_4 ; BE = 516.9–517.1 eV for V^{4+} in $(\text{VO})_2\text{P}_2\text{O}_7$.

Sample	$\text{V}2\text{P}_{3/2}$		$\text{V}^{5+}/\text{V}^{4+}$	P/V
	BE (eV)	A%		
VPO-2M	518.1	40	0.7	$\leq 1.0^a$
	516.9	60		
VPO-S-b	518.3	54	1.2	1.2
	517.0	46		
VPO-S-bt	518.3	50	1.0	1.2
	517.0	50		
VPO-S+2M	518.4	10	0.1	1.0
	517.1	90		
VPO-S+2Mt	518.7	13	0.1	1.0
	517.4	87		

^a A high charge effect, make difficult a more precise analysis of this sample. Similar results were observed after test.

Table 3

Catalytic activity results. Conversion of *n*-butane, maleic anhydride yield and selectivity for VPO-P-b, VPO-S-b and the modified VPO-S+2M catalysts during Step 3 (380 °C, 3.6 C₄/13.4 O₂).

Catalyst	Conversion (mol%)	Selectivity (mol%)	Yield in MA (mol%)
VPO-2M	11.3	0.0	0.0 ^a
VPO-P-b	33.2	49.5	16.4
VPO-S-b	14.6	67.7	9.9
VPO-S+2M	20.7	77.7	16.1

^a Only CO and CO₂ were produced.

studied the same DuPont catalysts, the amount of V⁵⁺ was higher in VPO-S (44 mol%) than in the just calcined catalyst (32 mol%) or in the precursor VPO-P (22 mol%). In VPO-S+2M catalyst, the P/V atomic ratio decreased to 1.0, confirming that a phase with a P/V atomic ratio lower than 1 had been deposited on the surface (P/V = 1.2 in VPO-S-b).

These results suggest that, after slurring the spent catalyst with solution containing P/V = 0.86, the catalyst surface was partly restructured, without heating, with decreasing amount of V⁵⁺ and restored P/V ratio close to 1.0.

3.3. Characterization of catalysts after catalytic testing

The catalytic properties of VPO-S-b and VPO-S-2M were studied (*vide infra*) and XRD, LRS and XPS techniques were used to study the catalysts after catalytic experiments (VPO-2Mt, VPO-S-bt and VPO-S-2Mt).

After the catalytic test, the state of VPO-2M became even more amorphous (Fig. 1). Only the phase attributed to (VO)₃(PO₄)₂·6H₂O (ICDD-JCPDS 49-1256) could be identified. XPS results were similar to those before the test. The presence of α₁-VOPO₄ besides (VO)₂P₂O₇ was observed by LRS in VPO-S-bt. α- and β-VOPO₄ besides (VO)₂P₂O₇ were detected in VPO-S+2Mt. In addition VOPO₄·2H₂O was observed in VPO-S-bt spectrum (Table 1). The XRD pattern of VPO-S-bt showed that (VO)₂P₂O₇ and V₂O₅ were still present, while only (VO)₂P₂O₇ was detected in VPO-S+2Mt (Table 1). The results of the XPS analysis of the catalysts after testing showed that there was little to no change of the P/V ratio and of the amount of V⁵⁺ (13 vs. 10% in VPO-S+2Mt and 54 vs. 50% in VPO-bt, Table 2).

3.4. Catalytic properties

Typical values of *n*-butane (X_{C₄}) conversion and selectivity to maleic anhydride (S_{MA}) for catalysts submitted to the operating conditions after Step 3 are presented in Table 3. These operating conditions are significantly more reusing than that practices in fixed bed reactors (~1.8% butane in air) and are closer to fluid bed commercial conditions C₄/O₂ = 3.6/13.4. The highest conversion of *n*-butane was exhibited by the precursor slurred in isobutanol (VPO-P-b) and activated *in situ* (X_{C₄} = 33.2 mol%). The low conversion (X_{C₄} = 14.6 mol%) observed for VPO-S-b increased slightly up to X_{C₄} = 20.7 mol% upon slurring with 2 monolayers of VPO. This is remarkable because the catalytic activity of VPO-2M alone was low (X_{C₄} = 11.3 mol%) and that no maleic anhydride was produced (only CO and CO₂). The selectivity to MA increased in the following order: VPO-P-b (49.5 mol%) < VPO-S-b (67.7 mol%) < VPO-S+2M (77.7 mol%). Though the selectivity to MA was null when using VPO-2M, the slurring of VPO-S under conditions similar to those used to prepare VPO-2M led to higher selectivity and yield. The latter increased from Y_{MA} = 9.9 (VPO-S-b) to 16.1 mol% (VPO-S+2M), which equals the yield obtained with the *in situ* activated precursor (16.4 mol%). The production rates for VPO-P, VPO-S and VPO-S+2M catalysts are shown in Fig. 2. The rate of *n*-butane conversion was higher at about 40% and the maleic anhydride production was

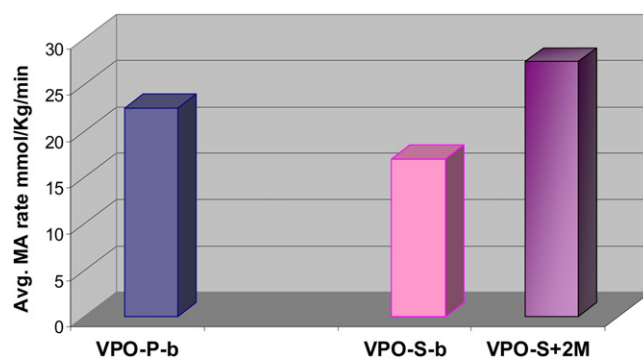


Fig. 2. Maleic anhydride production rates for VPO-P-b, VPO-S-b and modified VPO-S+2M catalysts.

higher at about 60% for VPO-S+2M compared to spent VPO-S-b. Therefore, the deposition of the two monolayers on the surface of VPO-S catalyst resulted in a significant recovery of activity and maleic anhydride productivity.

3.5. Possible reasons for VPO catalyst reactivation

Several mechanisms could account for the ageing of DuPont catalyst including upsets in the operating conditions and localized thermal excursions at the oxygen spargers, which could favour the gradual transformation of the already present VOPO₄ phases to β-VOPO₄. Though VOPO₄ forms could be active in the formation of MA from butenes, butadiene, furan [6,8,9], if these intermediates were formed, the formation of β-VOPO₄ is irreversible [5]. β-VOPO₄ is the ultimate form of VOPO₄ to which any allotropic VOPO₄ tends. Moreover its formation is indicative of the thickening of (VO)₂P₂O₇ platelets, which is one way of ageing of VPO catalysts. Indeed it was shown that by reoxidation of (VO)₂P₂O₇, thin platy crystals yielded δ or γ-VOPO₄ while prismatic crystals yielded β-VOPO₄ [20,21,26]. The loss of phosphorus, leading to the more facile reoxidation of (VO)₂P₂O₇, the presence of V₂O₅, which appears because of hydrolysis of VOPO₄, as well as of iron oxide, coming from abrasion of VPO particles onto the reactor wall [22,25], could also play detrimental roles. We cannot exclude that during the isobutanol procedure, some iron oxide and excess of phosphate could be washed away. Further experimental work is required to better discriminate the magnitude of each of these mechanisms.

VPO-P-b, which was more active under the same reaction conditions, contained only 7% of V⁵⁺, and VPO-S-2M, which was the most active catalyst, contained 13% of V⁵⁺. The high fraction of V⁵⁺ detected in VPO-S-b catalyst was in agreement with the VPO phases found by XRD and LRS (V₂O₅ and α₁-VOPO₄) (Tables 1 and 2). The principal consequence of this phase transformation, which led to the deactivation of VPO DuPont catalyst, was probably due to the high amount of V⁵⁺ formed on its surface with time-on-stream.

The improvement of catalytic performance of the deactivated catalyst can result from (i) a more appropriate distribution of V⁵⁺/V⁴⁺ ratio and P/V close to 1.0 and (ii) the disappearance of detrimental phases. XPS showed that a low amount of V⁵⁺ (V⁵⁺/V⁴⁺ = 0.1 instead of 1.2 for VPO-S-b), which did not change much after catalytic experiments, as the one found in the precursor VPO-P, was recovered, as well as the initial P/V = 1.0 (1.0 in fresh VPO). When VPO-S was refluxed in isobutanol, part of the detrimental V₂O₅ (and probably α-VOPO₄), and may be some excess phosphate, were washed out after filtration. Consequently the surface area increased (12 vs 8 m² g⁻¹ for VPO-S). The activity was lower than that of the calcined precursor VPO-P-b (X_{C₄} = 14.6 vs. 33.2%) but the selectivity to MA was quite high (67.7 vs. 49.5%).

In the case of VPO-S+2M, it is important to emphasize that the amount of vanadium (2 theoretical monolayers in the suspension) into which the VPO-S catalyst was added is very small as compared with the total amount of $(VO)_2P_2O_7$ in the catalyst. If all the vanadium deposited was converted to a (hypothetical) active VPO phase, the weight of this phase would represent at most 3.6% of the total weight of the VPO-S+2M catalyst. However, since the catalytic performance of VPO-S+2M is slightly higher than that of the *in situ* activated precursor, the surface of VPO-S could have been reloaded with VPO species close to those of $VOHPO_4 \cdot 0.5H_2O$. Indeed it is striking that the surface area is the same than that of VPO-P. Finally, finely tuning the P/V atomic ratio and the amount of the VPO phase deposited on deactivated DuPont catalysts could allow to optimize the recovery in activity and to improve further selectivity.

4. Conclusions

Firstly, the precursor and spent DuPont catalyst were submitted to a treatment consisting of slurring the particles in isobutanol. This treatment resulted in washing out potentially detrimental species, like vanadium oxide, which is formed by hydrolysis of $VOPO_4$ phases due to the high amount of water formed into the reaction (4 H_2O per one MA). It is not excluded that during this process iron oxide, excess phosphorous, and may be also certain forms of $VOPO_4$ like α - $VOPO_4$ were also eliminated. In accordance with these observations, and though the activity was lower than that exhibited by the *in situ* activated precursor VPO-P-b, the selectivity to MA was high (68 mol%).

In the next step, the particles of the spent catalyst were suspended in a vanadium containing isobutanol solution to which 85 wt.% phosphoric acid was added to achieve 2 theoretical monolayers of VPO (P/V = 0.86). Compared to the spent VPO-S-b catalysts, the maleic anhydride production increased by *ca.* 60% and the rate of butane transformation increased by *ca.* 40%. The selectivity to MA increased to 78%.

Analyses showed that most detrimental oxide species were no more present (XRD and LRS) and that V^{5+}/V^{4+} (about 10% of V^{5+}) and the P/V ratio (1.0) were lower (XPS). Therefore the treatment, which does not require a heating step, would result in the restructuring of the surface by the formation of an amorphous phase close to vanadyl phosphate hemihydrate. These species would enter the porous silica structure so as to make a thin layer coating the spent catalyst, and thus rejuvenating the VPO catalyst. Further experiments are in progress to confirm these findings, to improve the catalytic performance, and to determine the possible interactions with the active and selective phase.

The modified samples demonstrated a higher catalytic activity especially at higher *n*-butane concentrations in the feed, which corresponds to industrial reaction conditions in fluidized bed reactor and circulating fluidized bed reactors. The proposed methodology may be applicable to reactivate other catalytic formulations for other reactions.

References

- [1] V.V. Gulians, J.B. Benziger, S. Sundaresan, I.E. Wachs, A.M. Hirt, *Chemistry Letters* 62 (1999) 87.
- [2] X.-F. Huang, B.-H. Chen, B.-J. Liu, P.L. Silveston, C.-Y. Li, *Catalysis Today* 74 (2002) 121.
- [3] S. Albonetti, F. Cavani, F. Trifirò, P. Venturoli, G. Calestani, M. López Granados, J.L.G. Fierro, *Journal of Catalysis* 160 (1996) 52–64.
- [4] G.S. Patience, R.E. Bockrath, J.D. Sullivan, H.S. Horowitz, *Industrial and Engineering Chemistry Research* 46 (2007) 4374–4381.
- [5] E. Bordes, *Catalysis Today* 1 (1987) 499–526; E. Bordes, *Catalysis Today* 3 (1988) 163–174.
- [6] G. Centi, *Catalysis Today* 16 (1993) 5–26.
- [7] N. Ballarini, F. Cavani, C. Cortelli, M. Ricotta, F. Rodeghiero, F. Trifirò, C. Fumagalli, G. Mazzoni, *Catalysis Today* 117 (2006) 174–179.
- [8] E. Bordes, P. Courtine, *Journal of Catalysis* 57 (1979) 237–252.
- [9] J.C. Volta, *Académie des Sciences Paris, Series IIC, Chimie/Chemistry* 3 (2000) 717–723.
- [10] X.-F. Huang, C.Y. Li, B.-H. Chen, P.L. Silveston, *AIChE Journal* 48 (2002) 846–855.
- [11] L. Pérez-Moreno, S. Irusta, J. Soler, J. Herguido, M. Menéndez, *Chemical Engineering Journal* 147 (2009) 330–335.
- [12] E. Bordes, R. Contractor, *Topics in Catalysis* 3 (1996) 365–375.
- [13] G.J. Hutchings, C.J. Kiely, M.T. Sananes-Schulz, A. Burrows, J.C. Volta, *Catalysis Today* 40 (1998) 273–286.
- [14] J.C. Volta, C.J. Kiely, G.J. Hutchings, *Applied Catalysis A: General* 325 (2007) 194–197.
- [15] E. Kleimenov, H. Bluhm, M. Hävecker, A. Knop-Gericke, A. Pestryakov, D. Teschner, J.A. Lopez-Sanchez, J.K. Bartley, G.J. Hutchings, R. Schlögl, *Surface Science* 575 (2005) 181–188.
- [16] C. Cavallo, F. Cavani, S. Ligi, F. Trifirò, *Studies in Surface Science and Catalysis* 119 (1998) 925–930.
- [17] F. Cavani, D. De Santi, S. Luciani, A. Löfberg, E. Bordes-Richard, C. Cortelli, R. Leanza, *Applied Catalysis A: General* 376 (1–2) (2010) 66–75.
- [18] F. Cavani, S. Luciani, E. Degli Esposti, C. Cortelli, R. Leanza, *Chemistry: A European Journal* 16 (2010) 1646–1655.
- [19] P. Ruiz, Ph. Bastians, L. Caussin, R. Reuse, L. Daza, D. Acosta, B. Delmon, *Catalysis Today* 16 (1993) 99–111.
- [20] E. Kestemann, M. Merzouki, B. Taouk, E. Bordes, R. Contractor, *Preparation of catalysts VI*, in: G. Poncelet, et al. (Eds.), *Studies in Surface Science and Catalysis* 91 (1995) 707–716.
- [21] N. Duvauchelle, E. Kesteman, F. Oudet, E. Bordes, *Journal of Solid State Chemistry* 137 (1998) 311–324.
- [22] DuPont Industry, *Applied Catalysis A: General* 376 (2010) 1–3, and papers therein.
- [23] R.M. Contractor, D.I. Garnett, H.S. Horowitz, H.E. Bergna, G.S. Patience, J.T. Schwartz, G.M. Sisler, in: V. Cortés Corberán, S. Vic Bellón (Eds.), *New Developments in Selective Oxidation II*, Elsevier, Amsterdam, *Studies in Surface Science and Catalysis* 82 (1994) 233–242.
- [24] T.C. Watling, G. Deo, K. Seshan, I.E. Wachs, J.A. Lercher, *Catalysis Today* 28 (1996) 139–145.
- [25] N.F. Dummer, W. Weng, C. Kiely, A.F. Carley, J.K. Bartley, C.J. Kiely, G.J. Hutchings, *Applied Catalysis A: General* 376 (2009) 47–56.
- [26] N. Duvauchelle, E. Bordes, *Catalysis Letters* 57 (1999) 81–88.